Field-Oriented Control of an Induction Motor with Robust On-Line Tuning of Its Parameters

Toshihiko Noguchi, *Member, IEEE*, Seiji Kondo, *Member, IEEE*, and Isao Takahashi, *Fellow, IEEE*

Abstract—**This paper proposes new torque control of an induction motor, which is robust against primary resistance and adaptable to leakage inductance, magnetizing inductance, and secondary time constant. The control is based on flux feedback with a flux simulator. Since the simulator is based on a rotor current model, it is independent of the primary resistance, but uses the magnetizing inductance and secondary time constant values to estimate the flux. Parameter mismatch in the simulator detrimentally affects flux and torque responses. In order to compensate for degradation of the responses, an identifier for the magnetizing inductance and the secondary time constant is introduced. The identifier is insensitive to the primary resistance because it is based on instantaneous reactive power of the motor. Also, a leakage inductance identifier is introduced to achieve perfect compensation, which is robust against other parameters owing to instantaneous harmonic reactive power. To verify feasibility of the proposed technique, digital simulations and experimental tests have been conducted. The results have proven excellent characteristics of the drive system, which confirms validity of the scheme.**

Index Terms—**Induction motor, field-oriented control, parameter identification, leakage inductance, magnetizing inductance, secondary time constant, robustness, primary resistance.**

I. Introduction

FIELD-ORIENTED control of an induction motor has achieved a quick torque response, and has been applied in various industrial applications instead of a dc motor. In recent years, many research studies have been done on automated tuning of the motor parameters. Most of the conventional tuning techniques, however, were based on off-line parameter measurement [1]–[3]. They are effective to obtain automated and highly accurate adjustments of the motor parameters, but some problems still remain. First of all, the parameters which may vary during operation are not dynamically compensated. Secondly, the conventional techniques require some kinds of special operating patterns to measure the parameters. Finally, the off-line tuning itself is complicated and time consuming. Therefore, a concept of on-line identification ought to be introduced into the system to overcome the above problems [4]–[8]. The on-line identification technique enables to accomplish not only the automated and highly accurate measurement but also dynamic optimization of the parameters.

Paper IPCSD 96–35, approved by the Industrial Drives Committee of the IEEE Industry Applications Society for presentation at the 1996 International Conference on Power Electronics, Drives, and Energy Systems for Industrial Growth, New Delhi, India, January 8–12. Manuscript released for publication May 20, 1996.

The authors are with the Nagaoka University of Technology, Niigata 940-21, Japan.

Publisher Item Identifier S 0093-9994(97)00989-4.

This paper describes a novel torque control strategy of the induction motor, which has adaptability to leakage inductance, magnetizing inductance and a secondary time constant as well as robustness against primary resistance. The principle of the strategy is based on flux-feedback field orientation with a flux simulator and two robust identifiers for the motor parameters. One identifier is introduced into the system to compensate for parameter mismatch of the magnetizing inductance and the secondary time constant. It is insensitive to the primary resistance because it is based on instantaneous reactive power of the motor. In addition, the leakage inductance value, which is necessary for the above identifier, is estimated by the other identifier which is based on instantaneous harmonic reactive power. Consequently, the proposed method makes it possible to attain the fully automated on-line tuning of all parameters with robustness against the variation of the primary resistance. In what follows, theoretical analysis is developed, and results of computer simulations and experimental tests are presented.

II. Flux-Feedback Field-Oriented Control

Fig. 1 shows a configuration of a flux-feedback field-oriented controller to be studied. A secondary flux vector is estimated by a flux simulator of (1) in the system, and its block diagram is shown in Fig. 1(b). As shown in Fig. 1(a), instantaneous torque control can be achieved by a current controller using the estimated flux. Equations (2)–(4) show the control algorithms, and the current controller is constituted on rotating d–q coordinates.

$$\hat{\psi}_{2\alpha\beta} = \frac{\hat{M}}{1 + (p - j\omega_m)\hat{\tau}_2} i_{1\alpha\beta} \tag{1}$$

$$i^*_{1dq} = i^*_{1d} + j i^*_{1q} = G_{AFR}(|\psi_2|^* - |\psi_2|) + j\frac{T^*}{|\psi_2|^*} \tag{2}$$

$$i_{1dq} = \frac{\hat{\psi}_{2\alpha\beta}}{|\hat{\psi}_2|} i_{1\alpha\beta} \tag{3}$$

$$v^*_{1\alpha\beta} = \frac{\hat{\psi}_{2\alpha\beta}}{|\hat{\psi}_2|} v^*_{1dq} \tag{4}$$

where the variables and the parameters are defined as follows:

v_1	primary voltage vector;
i_1	primary current vector;
ψ_2	secondary flux vector;
T	output torque;
G_{AFR}	transfer function of an automatic flux regulator (PI controller);
ω	rotating speed of the d–q coordinates;

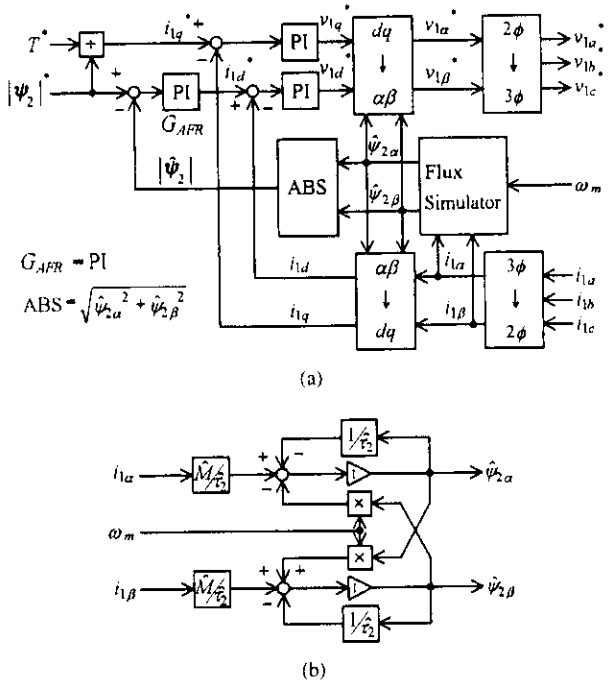

Fig. 1. Configuration of field-oriented control system:.(a) Block diagram of flux-feedback field-oriented controller. (b) Block diagram of secondary flux simulator.

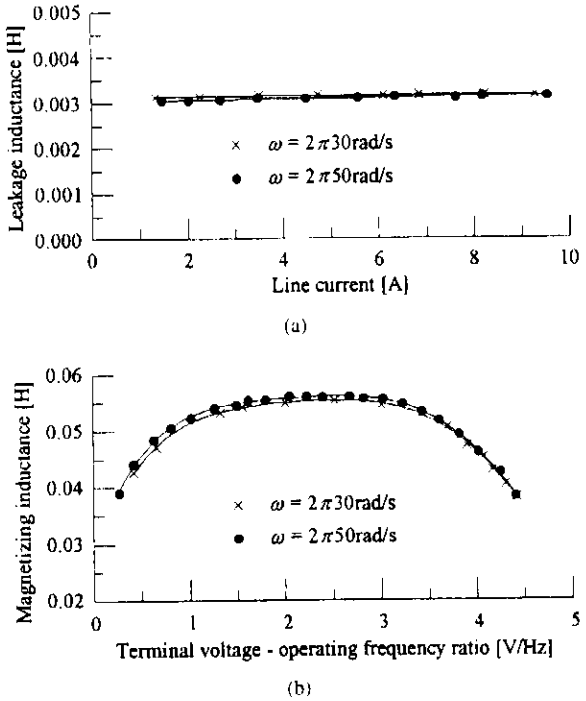

Fig. 2. Inductances of test induction motor. (a) Leakage inductance. (b) Magnetizing inductance.

ω_m	rotating speed of a rotor;
R_1	primary resistance;
R_2	secondary resistance;
L_{11}	primary self inductance;
L_{22}	secondary self inductance;
M	magnetizing inductance;
$\ell = \frac{L_{11}L_{22}-M^2}{L_{22}}$	leakage inductance;
$\tau_2 = L_{22}/R_2$	secondary time constant;
p	differential operator;
j	imaginary unit;
$\hat{x}$	estimated value of x;
x^*	command value of x;
$\|x\|$	amplitude of x;
$\mathrm{Im}(x)$	imaginary part of x;
$\bar{x}$	complex conjugate of x;
$x_{\alpha\beta}$	vector x on stator (α–β) coordinates;
x_{dq}	vector x on the flux (d–q) coordinates.

The simulator shown in Fig. 1(b) is based on a rotor current model, which requires detecting $i_{1\alpha\beta}$ and ω_m. The model can estimate $\hat{\psi}_{2\alpha\beta}$ all over the speed range including zero speed because it does not include pure integrators. As shown in Fig. 1(a), on the d–q coordinates rotating synchronously with the secondary flux, the flux amplitude and the output torque can be controlled by manipulating the flux component current i_{1d} and the torque component current i_{1q} respectively. Since it is necessary to control each current component, the detected $i_{1\alpha\beta}$ and the voltage command v_{1dq}^* are transformed by using $\hat{\psi}_{2\alpha\beta}$. Therefore, if the simulator estimates $\hat{\psi}_{2\alpha\beta}$ with an error, the current control on the d–q coordinates can not be carried out completely. This prevents the system from controlling the flux and the output torque without steady-state errors nor transient phenomena. Parameter mismatch of $\hat{M}$ and $\hat{\tau}_2$ brings the estimation error. The parameter mismatch of $\hat{M}$ is caused by magnetic saturation (nonlinearity), whereas that of $\hat{\tau}_2$ is caused by the magnetic saturation and thermal variation. Fig. 2 shows examples of the inductances which were measured for a test induction motor. It is found that ℓ is almost constant, but M varies widely according to the operating condition. Since the tested motor is a standard squirrel cage induction motor, ℓ hardly varies with the line current. In the cases of motors with a double squirrel cage or closed rotor slots, however, ℓ can vary with the operating condition, especially with the line current.

III. Principle of Robust Identification of Parameters

A. Identification of Leakage Inductance

Since parameter mismatch of the leakage inductance $\hat{\ell}$ causes identification errors of $\hat{M}$ and $\hat{\tau}_2$, which are described in the next section, identification of $\hat{\ell}$ should not be affected by any other parameters to achieve perfect parameter tuning.

An equivalent circuit of the induction motor in a steady state is given in Fig. 3(a), which is for a fundamental angular frequency ω. For much higher angular frequency $\omega_h \gg \omega$, however, the circuit can be simplified as shown in Fig. 3(b). Therefore, the effects of M and ω_m can be neglected for the higher component. By using harmonic vectors v_{1h} and i_{1h} with the angular frequency of ω_h, $\hat{\ell}$ can be identified as follows. As shown in Fig. 4, v_{1h} is intentionally superposed on the primary voltage vector command v_{1dq}^*. Since it is important to extract i_{1h} from i_{1dq} as precisely as possible, a digital filter with a bandpass characteristic is used. The digital filter is represented by the following transfer function, of which coefficients are

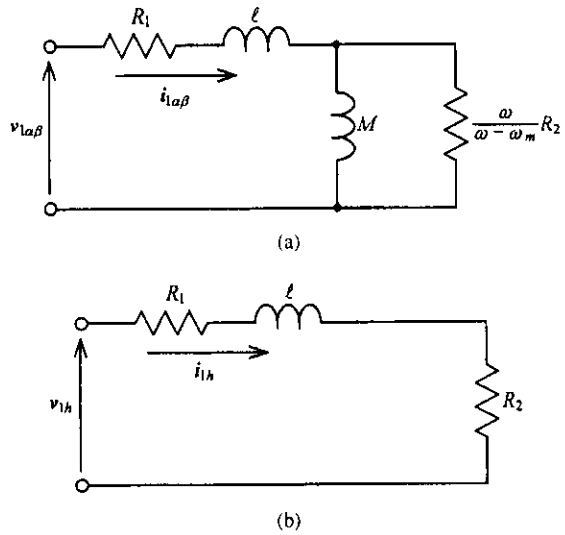

Fig. 3. Equivalent circuits of induction motor. (a) Equivalent circuit for fundamental component. (b) Equivalent circuit for harmonic component.

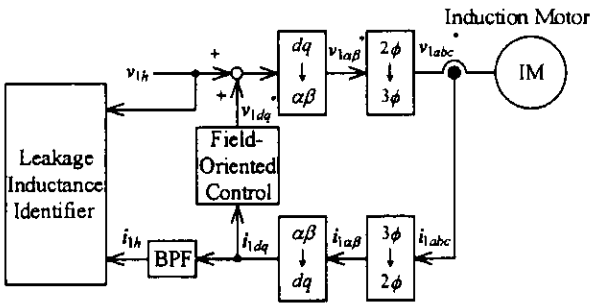

Fig. 4. Leakage inductance identifier and field-oriented control system.

specified by a central frequency, a quality factor and a gain.

$$H(z) = \frac{b_1 z^{-1} - b_2 z^{-2}}{1 - a_1 z^{-1} + a_2 z^{-2}}. \tag{5}$$

When v_{1h} and i_{1h} are obtained as described above, instantaneous harmonic reactive power Q_h can be calculated by

$$Q_h = \mathrm{Im}(v_{1h}\bar{i}_{1h}). \tag{6}$$

It is known that (6) does not require any motor parameters and is independent of motor conditions. As shown in Fig. 3(b), a circuit equation for the harmonic component is expressed as

$$v_{1h} = (R_1 + R_2 + p\ell)i_{1h}. \tag{7}$$

Substituting (7) into (6), R_1 and R_2 are canceled out perfectly, and the following expression is derived.

$$Q_h = \ell\ \mathrm{Im}(pi_{1h}\bar{i}_{1h}). \tag{8}$$

Equations (6) and (8) are insensitive to both R_1 and R_2, whereas (8) requires the value ℓ. If there exists parameter mismatch in ℓ, (8) has an error; hence ℓ in (8) should be replaced with an estimated value $\hat{\ell}$ as

$$\hat{Q}_h = \hat{\ell}\ \mathrm{Im}(pi_{1h}\bar{i}_{1h}). \tag{9}$$

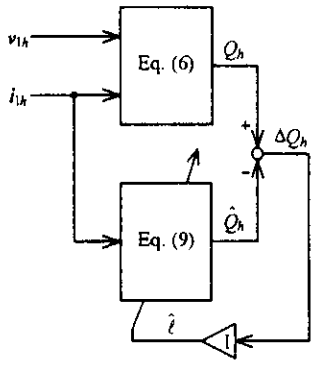

Fig. 5. Leakage inductance identifier.

The error between (8) and (9) can be calculated in the steady state as

$$\Delta Q_h = \omega_h(\ell - \hat{\ell})|I_{1h}|^2. \tag{10}$$

Since $\omega_h \neq 0$, $\Delta Q_h = 0$ if and only if $\hat{\ell} = \ell$. Therefore, it is possible to identify $\hat{\ell}$ uniquely by using ΔQ_h under any conditions.

Fig. 5 shows a configuration of a leakage inductance identifier. The value of Q_h calculated by (6) is a reference value, and $\hat{Q}_h$ estimated by (9) is a theoretical value. The error ΔQ_h between them dynamically adjusts $\hat{\ell}$. Because the identifier utilizes an integrator as an identification algorithm, it is not suitable for estimating $\hat{\ell}$ which may rapidly vary with the line current as mentioned before. However, the proposed technique can identify $\hat{\ell}$ uniquely and independently of other parameters in the steady state.

Since v_{1h} is a high frequency vector, winding resistance may increase owing to skin effects. By using the instantaneous harmonic reactive power, however, increases of R_1 and R_2 can be neglected including the skin effects as well as thermal variations, which is also an advantage of the proposed technique.

B. Identification of Magnetizing Inductance and Secondary Time Constant

In what follows, an identification technique for the magnetizing inductance $\hat{M}$ and the secondary time constant $\hat{\tau}_2$, which is never affected by the variation of the primary resistance R_1, is discussed. The identified leakage inductance value $\hat{\ell}$, which was described in the previous section, is utilized in the identifier for $\hat{M}$ and $\hat{\tau}_2$.

A conventional technique is based on comparison between the rotor current model given in (1) and a stator voltage model given in (11)

$$\psi_{2\alpha\beta} = \frac{1}{p}(v_{1\alpha\beta} - R_1 i_{1\alpha\beta}) - \ell i_{1\alpha\beta}. \tag{11}$$

Equation (11) is utilized as a reference model, but it requires not only R_1 but also an integrator. Consequently, the identification of $\hat{M}$ and $\hat{\tau}_2$ in (1) becomes incomplete because the integrator probably accumulate the error of R_1.

In order to avoid the above problem, instantaneous reactive power Q of the motor is introduced. The reactive power Q is

defined by the following equation on the α-β coordinates.

$$Q = \mathrm{Im}(v_{1\alpha\beta}\bar{i}_{1\alpha\beta}). \tag{12}$$

The right-hand side of (12) can be evaluated statically by using the detected $v_{1\alpha\beta}$ and $i_{1\alpha\beta}$, which means that it requires no integrators. It always provides a true value because no parameters of the motor are used. On the other hand, substituting $v_{1\alpha\beta}$ of (11) into (12), Q can be rewritten as follows:

$$Q = \mathrm{Im}(p\psi_{2\alpha\beta}\bar{i}_{1\alpha\beta} + \ell p i_{1\alpha\beta}\bar{i}_{1\alpha\beta}). \tag{13}$$

The term of R_1 in (11) is canceled out perfectly in the derivation [6]–[8]; hence (13) is independent of R_1. Equation (13) requires $\psi_{2\alpha\beta}$, however, which may be estimated by the flux simulator shown in Fig. 1(b). The simulator uses the values of $\hat{M}$ and $\hat{\tau}_2$. The parameter mismatch possibly causes an error in (13); hence it is feasible to replace (13) with (14).

$$\hat{Q} = \mathrm{Im}(p\hat{\psi}_{2\alpha\beta}\bar{i}_{1\alpha\beta} + \hat{\ell} p i_{1\alpha\beta}\bar{i}_{1\alpha\beta}). \tag{14}$$

The difference between (13) and (14) can be derived as

$$\Delta Q = \mathrm{Im}\{p(\psi_{2\alpha\beta} - \hat{\psi}_{2\alpha\beta})\bar{i}_{1\alpha\beta} + (\ell - \hat{\ell})(p i_{1\alpha\beta}\bar{i}_{1\alpha\beta})\}. \tag{15}$$

Since the on-line tuning technique presented in this paper aims at providing parameter compensation capability in the steady state, instantaneous variables can be replaced as $p \rightarrow j\omega$, $\psi_{2\alpha\beta} \rightarrow \Psi_2$, $\hat{\psi}_{2\alpha\beta} \rightarrow \hat{\Psi}_2$, and $i_{1\alpha\beta} \rightarrow I_1$ in (1) and (15), where the upper-case variables represent phasors. Thus, ΔQ can be calculated as

$$\Delta Q = \omega\left[\frac{M - \hat{M} + (\omega - \omega_m)^2(M\hat{\tau}_2^2 - \hat{M}\tau_2^2)}{\{1 + (\omega - \omega_m)^2\hat{\tau}_2^2\}\{1 + (\omega - \omega_m)^2\tau_2^2\}} + \ell - \hat{\ell}\right] \times |I_1|^2. \tag{16}$$

It is recognized that there are infinitely many solutions which can make ΔQ zero; hence each parameter can not be identified uniquely without any restrictions. Assuming no-load conditions and that $\hat{\ell}$ has converged to a true value by using the identification technique discussed in the previous section, (16) is simplified as

$$\Delta Q = \omega(M - \hat{M})|I_1|^2. \tag{17}$$

It is found that $\Delta Q = 0$ if and only if $\hat{M} = M$ unless $\omega = 0$. In other words, it is possible to identify $\hat{M}$ uniquely by using ΔQ under no-load conditions. The magnetizing inductance M varies rapidly with the flux amplitude during field weakening operation. Because the amplitude varies according to the operating speed in the field weakening region, the identifier can properly estimate $\hat{M}$ unless the speed is suddenly changed.

Assuming that the identification of M has finished on the basis of the above process, that is $\hat{M} = M$, (16) can be rewritten as

$$\Delta Q = \frac{\omega(\omega - \omega_m)^2 M(\hat{\tau}_2 - \tau_2)(\hat{\tau}_2 + \tau_2)}{\{1 + (\omega - \omega_m)^2\hat{\tau}_2^2\}\{1 + (\omega - \omega_m)^2\tau_2^2\}}|I_1|^2. \tag{18}$$

It is found that $\Delta Q = 0$ if and only if $\hat{\tau}_2 = \tau_2$ unless $\omega = 0$ nor $\omega = \omega_m$. Therefore, it is possible to identify $\hat{\tau}_2$ uniquely by using ΔQ with the exception of direct current exiting or no-load conditions.

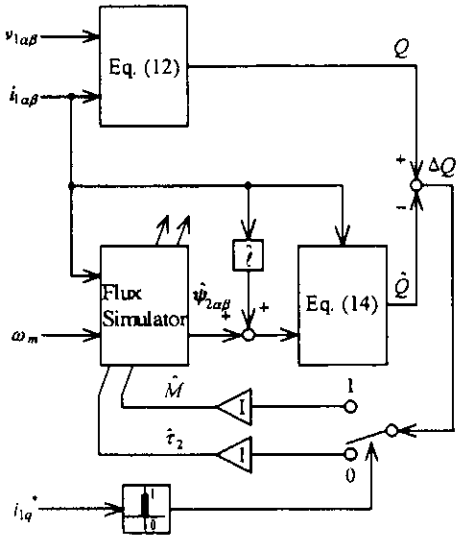

Fig. 6. Magnetizing inductance and secondary time constant identifier.

TABLE I
RATED VALUES AND NOMINAL PARAMETERS OF TESTED MOTOR

Rated output	1.5[kW]	ℓ	3.1[mH]
Rated torque	8.63[Nm]	M	51.0[mH]
R_1	0.542[Ω]	$\lvert\Psi_2\rvert^*$	0.427[Wb]
R_2	0.536[Ω]	Pole number	4[pole]

Fig. 6 shows a block diagram of the magnetizing inductance and secondary time constant identifier, which is insensitive to the primary resistance. The identifier is based on a parallel-type model reference adaptive system. Equation (12) is a reference model, and the flux simulator and $\hat{Q}$ of (14) constitute a mathematical model. The error ΔQ is utilized to adjust $\hat{M}$ and $\hat{\tau}_2$ in the flux simulator. Two integrators are employed as identification algorithms owing to the steady-state parameter compensation as mentioned before. They are switched complementarily by using the torque component current command i_{1q}^*. Identification algorithm for $\hat{M}$ is selected when the motor is under no-load conditions, whereas that for $\hat{\tau}_2$ is selected under loaded conditions. Simultaneous identification of $\hat{M}$ and $\hat{\tau}_2$ requires further study, but the proposed technique is a practical and easy way to identify $\hat{M}$ and $\hat{\tau}_2$ independently of R_1. When $\omega = 0$ or $\omega = \omega_m$, each identification algorithm holds a value which has been integrated as $\hat{M}$ or $\hat{\tau}_2$, and it does not diverge. Since ΔQ is proportional to the operating frequency ω as shown in (16), convergence time of the identifier becomes longer at low speeds. Therefore, the gains of the two integrators are changed in inverse proportion to the operating speed.

IV. DIGITAL SIMULATION AND RESULTS

A digital simulation was conducted to examine robustness against the primary resistance and adaptability to the leakage inductance, the magnetizing inductance and the secondary time constant. The parameters of the induction motor are shown in Table I, and its output torque was controlled at a constant rotating speed of 1000 r/m. The harmonic voltage vector and

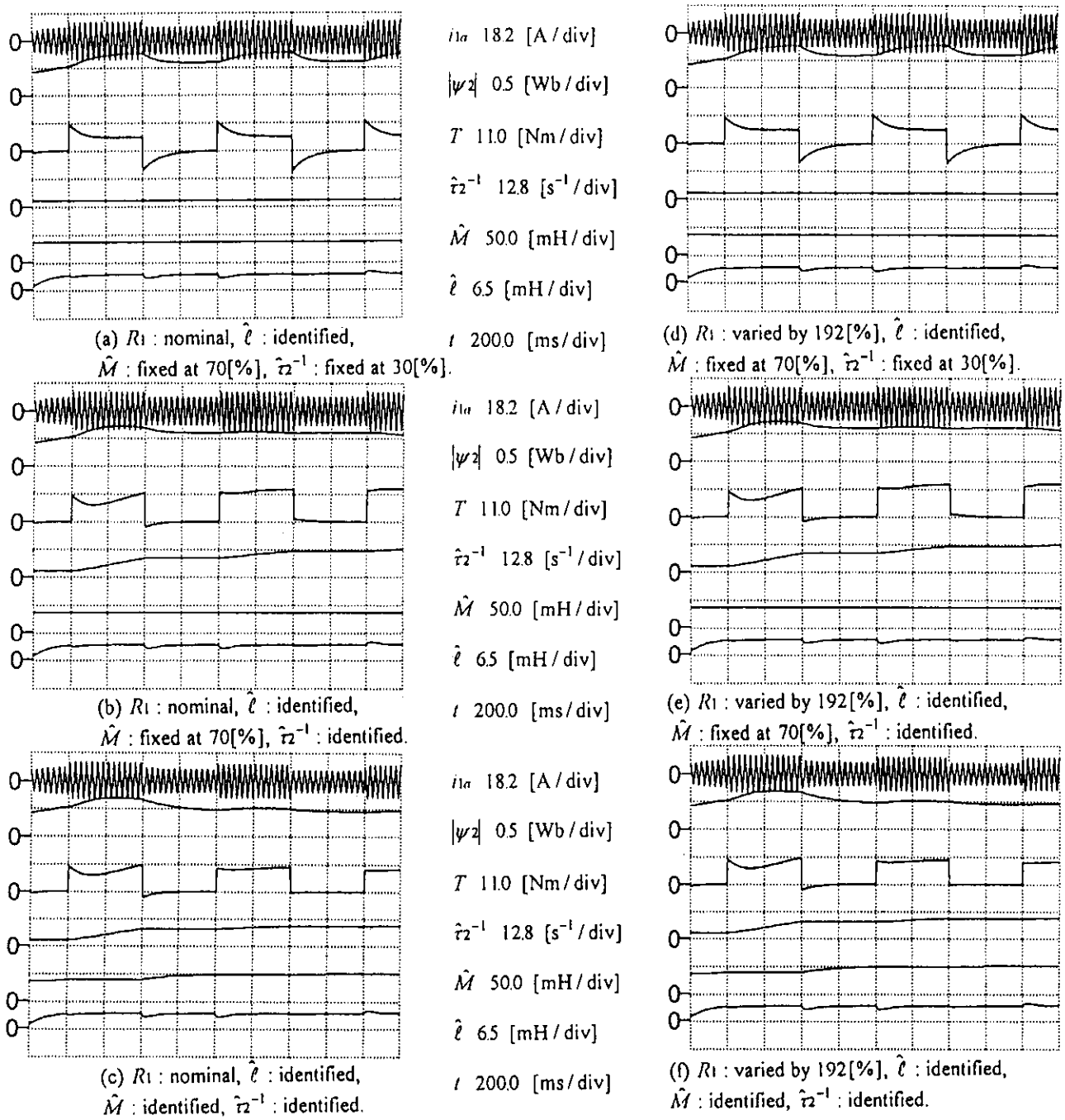

Fig. 7. Characteristics of parameter identification and torque control (simulation results).

the parameters of the digital filter (central frequency: 303.5 Hz; quality factor: 8.0; gain: 8.0) utilized for the leakage inductance identification are shown below:

$$v_{1h} = 8.0e^{j2\pi 303.5t} \tag{19}$$

$$a_1 = 1.9782;\ a_2 = 0.9878;\ b_1 = 0.0974;\ b_2 = 0.0974. \tag{20}$$

Fig. 7 shows step torque responses for 100% torque command, and the command is intermittently changed at low frequency (1.25 Hz). Condition of each simulation is described in its caption. The leakage inductance is simultaneously identified in every case. As shown in every figure, the identification of $\hat{\ell}$ is performed in about 200 ms, and is found to be robust against any other parameters and operating conditions. Small deviations of $\hat{\ell}$ are observed when the output torque steps up and down, which is owing to transient characteristics of the digital filter. Comparing Fig. 7(a)–(c) with Fig. 7(d)–(f), it is found that the proposed method is insensitive to R_1. It is because the field-oriented control system basically employs the rotor current model and the proposed identification techniques are based on the instantaneous reactive power of the motor. The parameter mismatch of $\hat{M}$ and $\hat{\tau}_2$ in the flux simulator causes transient phenomena in both flux and torque responses. Fig. 7(a) and (d) shows degradation of the responses. The parameter mismatch ought to be compensated independently of

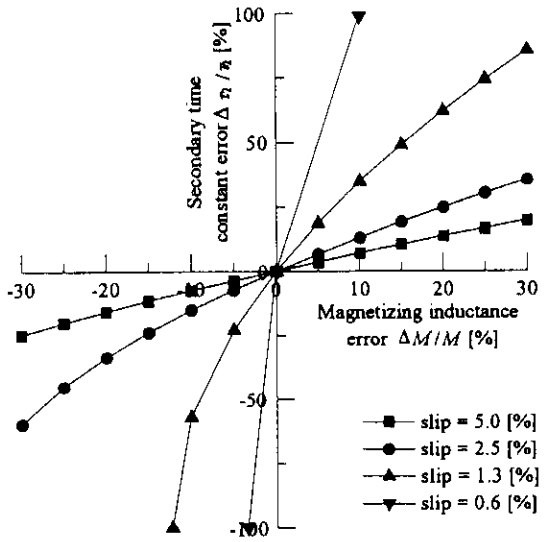

Fig. 8. Relation between errors of magnetizing inductance and secondary time constant.

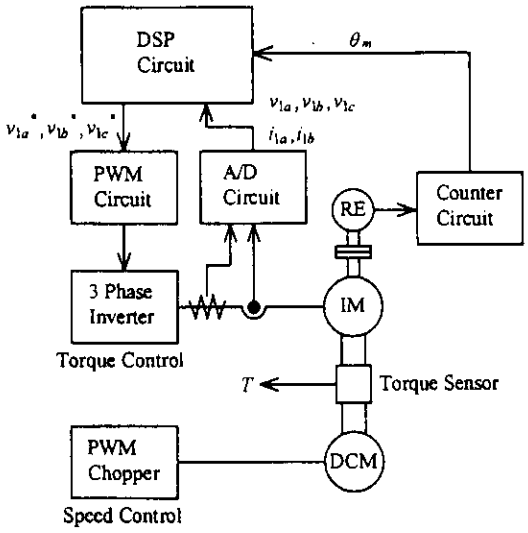

Fig. 9. Experimental system.

R_1 to improve the responses. On the other hand, when the only $\hat{\tau}_2$ is identified with allowing the parameter mismatch of $\hat{M}$ as shown in Fig. 7(b) and (e), the identification characteristics are not improved. The reason why the transient phenomena have remained in the responses is that unique convergence of $\hat{\tau}_2$ can not be certified in (16) unless $\hat{M}$ is identified. Assuming that $\Delta M = M - \hat{M}$ and $\Delta\tau_2 = \tau_2 - \hat{\tau}_2$ after the identifier has converged, that is $\Delta Q = 0$ in (16), the relation between ΔM and $\Delta\tau_2$ can be derived as

$$\Delta\tau_2 = \sqrt{\left(1 + \frac{\Delta M}{M}\right)\tau_2^2 + \frac{\Delta M}{(\omega - \omega_m)^2 M}} - \tau_2. \qquad (21)$$

Fig. 8 shows several plots of ΔM against $\Delta\tau_2$ according to (21). It is known that the parameter mismatch of $\hat{M}$ detrimentally affects the identification of $\hat{\tau}_2$. Therefore, the identification of $\hat{M}$ is essential for the unique convergence of $\hat{\tau}_2$. When both $\hat{M}$ and $\hat{\tau}_2$ are identified as shown in Fig. 7(c) and (f), the flux and torque responses are successfully improved with their convergence to the true values. Thus, quick torque responses are obtained without any transient oscillations and steady-state errors.

V. Experimental System and Results

A. Outline of Experimental System

Experimental tests were carried out to confirm feasibility of the proposed scheme. Fig. 9 shows a schematic diagram of an experimental system. The system consists of an inverter fed induction motor connected with a chopper fed dc motor. Parameters of a tested three-phase induction motor are same as those shown in Table I.

A fully digitized software control system was developed for the induction motor. Control and identification programs were executed completely by DSP (TMS320C50-40 MHz) software, and the control program was proceeded in 103 μs for every control period, while the program concerning the leakage inductance identifier which dealt with higher frequency signals was performed in every 51.5 μs. Specification of the harmonic voltage vector and the digital filter was same as described in (19) and (20). The output torque of the induction motor was controlled in a same way as that of the simulations. The mechanical rotating speed was regulated constant at 1000 r/m by the chopper fed dc motor. The shafts of the two motors are coupled with a strain-gage torque sensor. The actual output torque of the induction motor can be observed with the sensor.

B. Experimental Results

Fig. 10 shows experimental results of the above system. The experiments were conducted under the same conditions as those of the simulations. The primary resistance was varied by inserting external resisters of 0.5 Ω. As shown in every figure, $\hat{\ell}$ was identified independently of other parameters and operating conditions as well as the simulation results. In addition, characteristics of the torque response and the identification were found to be insensitive to R_1 comparing Fig. 10(a)–(c) with Fig. 10(d)–(f).

As shown in Fig. 10(a) and (d), transient phenomena were measured in the torque responses owing to the parameter mismatch of $\hat{M}$ and $\hat{\tau}_2$, and the steady-state output torque was decreased by approximately 50%.

On the other hand, improvement of the torque response was confirmed by Fig. 10(c) and (f) as follows. Transient phenomena in the responses were observed at the beginning of the identification because there had been parameter mismatch of $\hat{M}$ and $\hat{\tau}_2$ in their initial values. However, the identification started automatically, and each of $\hat{M}$ and $\hat{\tau}_2$ converged to a certain constant value. Comparing Fig. 10(c) with Fig. 7(c) with respect to $\hat{\tau}_2$, $\hat{\tau}_2$ estimated in the experimental test was approximately 80% of the nominal value. It is considered that the nominal value included nearly 20% errors because it had been evaluated by using an L-type equivalent circuit with thermal conversion. After convergence, it is known that the torque responses were successfully improved without any transient oscillations and steady-state errors. The torque

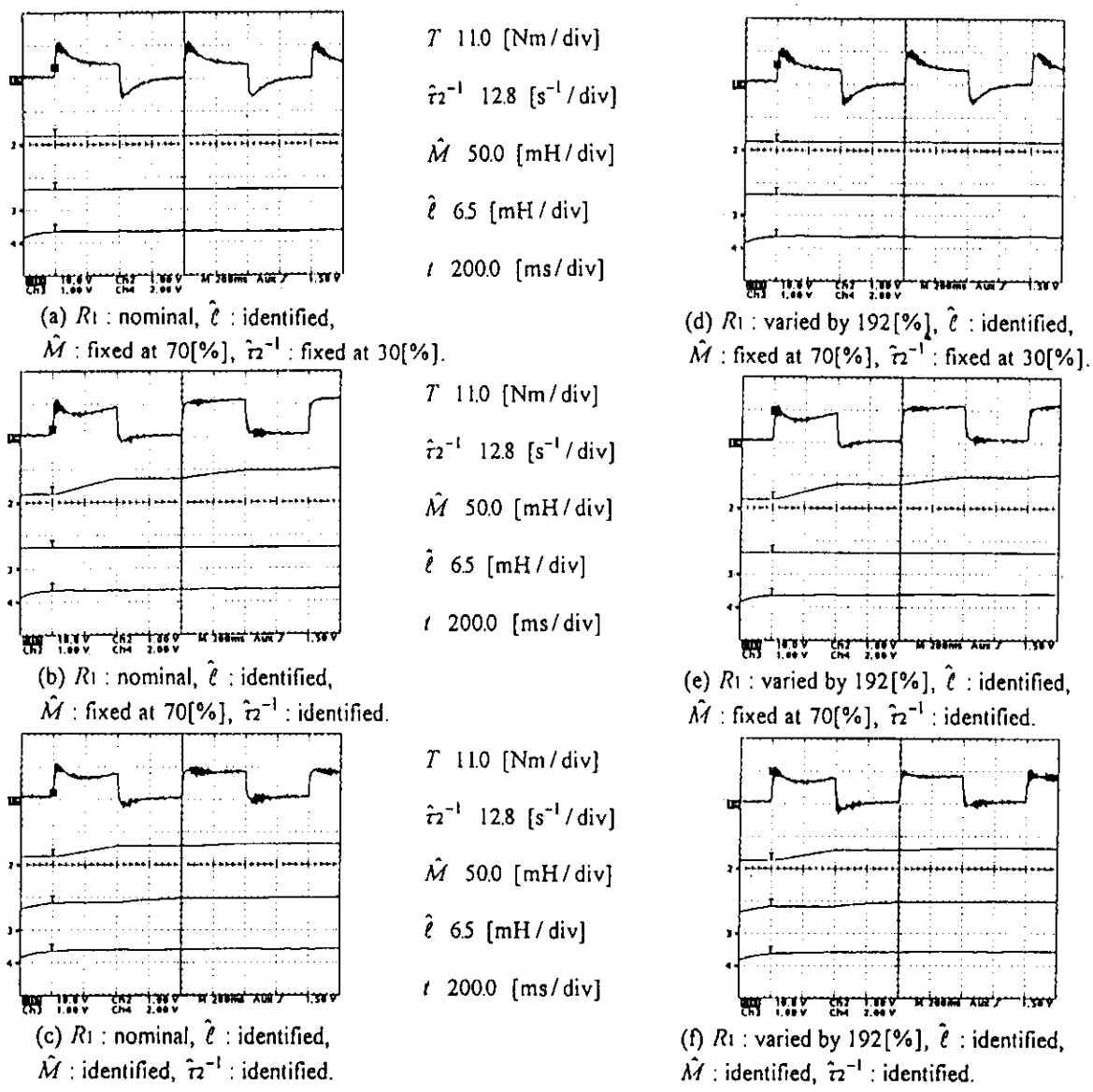

Fig. 10. Characteristics of parameter identification and torque control (experimental results).

response time was about 3 ms, and the performance was almost same as that of a dc motor. Furthermore, the variation of R_1 did not affect the compensation process as shown in Fig. 10(f).

VI. Conclusion

A torque control strategy of an induction motor with robustness against primary resistance and adaptability to leakage inductance, magnetizing inductance and a secondary time constant has been proposed. In this paper, results of theoretical analysis, digital simulations and experimental tests have been presented. Flux-feedback field-oriented control is robust against the variation of the primary resistance because its flux simulator is based on a rotor current model. Parameter mismatch of the magnetizing inductance and the secondary time constant in the simulator, however, detrimentally affects the control performance. Introducing a robust identifier, the parameter mismatch can be compensated completely without sensitivity to the primary resistance. The identifier is based on instantaneous reactive power of the motor, and it can automatically and uniquely identify the magnetizing inductance and the secondary time constant. Moreover, a leakage inductance identification technique has been described. The identified leakage inductance value is utilized in the above identifier to achieve perfect parameter tuning. The leakage inductance identifier is almost insensitive to any other parameters and operating conditions because it is based on instantaneous harmonic reactive power. The proposed techniques are expected to make induction motor drives completely free from adjustments of their parameters.

References

[1] C. Wang, D. W. Novotny, and T. A. Lipo, "An automated rotor time constant measurement system for indirect field-oriented drives," *IEEE Trans. Ind. Applicat.*, vol. IA-24, pp. 151–159, 1988.

[2] A. Gastli, M. Iwasaki, and N. Matsui, "An automated equivalent circuit parameter measurements of an induction motor using V/F PWM inverter," in *IPEC-Tokyo Conf. Rec.*, 1990, pp. 659–666.

[3] M. Akiyama, K. Kobayashi, I. Miki, and M. A. El-Sharkawi, "Auto-tuning method for vector controlled induction motor drives," in *IPEC-Yokohama Conf. Rec.*, 1995, pp. 789–794.
[4] J. Holtz and T. Thimm, "Identification of the machine parameters in a vector controlled induction motor drive," in *IEEE-IAS Ann. Meet. Conf. Rec.*, 1989, pp. 601–606.
[5] J. Moreira, K. Hung, T. Lipo, and R. Lorenz, "A simple and robust adaptive controller for detuning correction in field oriented induction machines," in *IEEE-IAS Ann. Meet. Conf. Rec.*, 1991, pp. 397–403.
[6] L. J. Garcés, "Parameter adaption for the speed-controlled static AC drive with a squirrel-cage induction motor," *IEEE Trans. Ind. Applicat.*, vol. IA-16, pp. 173–178, 1980.
[7] K. Tungpimolrut, F. Peng, and T. Fukao, "Robust vector control of induction motor without using stator and rotor circuit time constants," in *IEEE-IAS Ann. Meet. Conf. Rec.*, 1993, pp. 521–527.
[8] T. Noguchi, S. Kondo, and I. Takahashi, "Robust torque control of induction motor against variations of primary and secondary resistances," in *IPEC-Tokyo Conf. Rec.*, Yokohama, Japan, 1995, pp. 1163–1168.

Toshihiko Noguchi (M'95) was born in Kuwana, Japan, on October 23, 1959. He received the B.S. degree in electrical engineering from Nagoya Institute of Technology, Nagoya, Japan, in 1982, and the M.S. and Ph.D. degrees in 1986 and 1996, both in electrical and electronic systems engineering, from Nagaoka University of Technology, Niigata, Japan.

In 1982, he joined the Toshiba Corporation, Tokyo, Japan. He was a Lecturer at the Gifu National College of Technology, Gifu, Japan, from 1991 to 1993, and a Research Associate of electrical and electronic systems engineering at the Nagaoka University of Technology from 1994 to 1995. Since 1996, he has been an Associate Professor, Nagaoka University of Technology. His research interests are in static converters and motor drives.

Dr. Noguchi is a member of the Institute of Electrical Engineering of Japan.

Seiji Kondo (M'91) was born in Okazaki, Japan, on June 9, 1950. He received the B.S. degree in electronics engineering from Nagoya University, Nagoya, Japan, in 1973, and the Ph.D. degree in engineering from University of Tokyo, Tokyo, Japan, in 1991.

He jointed Hitachi Ltd., Tokyo, in 1973. From 1979 to 1991, he worked at the Institute of Industrial Science, University of Tokyo, where his research activities included the application of modern control theory to motor drives. He is currently an Associate Professor, Department of Electrical and Electronic Systems Engineering, Nagaoka University of Technology, Niigata, Japan. His interests are smart control techniques for power electronics and drives.

Dr. Kondo is a member of the Institute of Electrical Engineering of Japan.

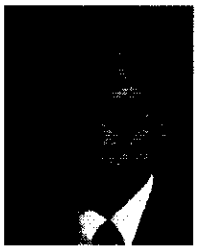

Isao Takahashi (M'81–SM'91–F'95) was born in Niitsu, Japan on March 10, 1942. He received the B.S., M.S. and Ph.D. degrees in electrical engineering from Tokyo Institute of Technology, Japan, in 1966, 1968, and 1971, respectively.

He was a Research Associate, Tokyo Institute of Technology, from 1971 to 1975, and an Associate Professor, Utsunomiya University, from 1975 to 1978. From 1978 to 1988, he was an Associate Professor of electrical and electronic systems engineering, Nagaoka University of Technology, Niigata, Japan. He was a Visiting Associate Professor at the University of Wisconsin, Madison, in 1982. Since 1988, he has been a professor at Nagaoka University of Technology. His research interests include electric power control, flywheel energy storage, active power filters, and high-performance servo drives.

Dr. Takahashi is also a member of the Institute of Electrical Engineering of Japan.